sustainability

MDPI

Article

Carbon Chemistry in the Mainstream of Kuroshio Current in Eastern Taiwan and Its Transport of Carbon into the East China Sea Shelf

Baoxiao Qu [1,2,3,*], Jinming Song [1,2,3,*], Huamao Yuan [1,2,3], Xuegang Li [1,2,3] and Ning Li [1,2,3]

1 Key laboratory of Marine Ecology and Environmental Sciences, Institute of Oceanology, Chinese Academy of Sciences, Qingdao 266071, China; yuanhuamao@qdio.ac.cn (H.Y.); lixuegang@qdio.ac.cn (X.L.); lining@qdio.ac.cn (N.L.)

2 University of Chinese Academy of Sciences, Beijing 100049, China

3 Function Laboratory of Marine Ecology and Environmental Sciences, Qingdao National Laboratory of Marine Science and Technology, Qingdao 266237, China

* Correspondence: qubx@qdio.ac.cn (B.Q.); jmsong@qdio.ac.cn (J.S.); Tel.: +86-532-82898583 (J.S.)

Received: 19 January 2018; Accepted: 7 March 2018; Published: 13 March 2018

Abstract: Comprehensive carbon chemistry data were measured from the mainstream of Kuroshio, off eastern Taiwan, in May 2014. Results indicated that variations of pH@25 °C, POC, Ω_{Ca}, DIC, pCO$_2$ and RF were closely related to the characteristics of various water types. Phytoplankton photosynthesis played important roles in DIC variation in Kuroshio Surface Water (KSW), whereas the DIC variation in Kuroshio Subsurface Water (KSSW) was probably influenced by the external transport of DIC-enriched water from the South China Sea. Vertical profiles of hydrological parameters and carbonate species indicated that the Kuroshio Current off eastern Taiwan could intrude into the ECS shelf as far as 27.9° E, 125.5° N in spring. What is more, the KSW, KSSW and Kuroshio Intermediate Water (KIW) could convey DIC into the East China Sea (ECS) with flux of 285, 305 and 112 Tg C/half year (1 Tg = 10^{12} g), respectively. The relevant flux of POC was 0.16, 2.93 and 0.04 Tg C/half year, respectively. Consequently, the intrusion of Kuroshio could probably exert a counteracting influence on the potential of CO_2 uptake in the ECS, which needs further study.

Keywords: carbon dioxide; dissolved inorganic carbon; continental shelf; east china sea; Kuroshio; eastern Taiwan

1. Introduction

Human activities have produced a 45% increase of carbon dioxide (CO_2) in the atmosphere, from 280 ppm in 1750 to 405 ppm in 2017. The ocean plays a significant role in uptaking anthropogenic CO_2, since about one-third of anthropogenic CO_2 is stored in the ocean [1]. Characteristics of continental shelves and/or marginal seas in the global carbon budget have been investigated substantially during recent decades, mainly because of their potential capacity for absorbing the ever-increasing atmospheric CO_2 value and regulating the global CO_2 inventory [1–4].

The East China Sea (hereafter referred to as ECS) is known as one of the largest temperate continental shelf seas in the world, which covers a shelf area (water depth < 200 m) of about 0.5×10^6 km^2. Being as the transition zone between the largest continent—Eurasia—and the biggest ocean—the Pacific—the ECS has always been considered a significant sink for atmospheric CO_2 [5–12]. In the 1990s, Japanese scientists first reported the CO_2 sink/source terms of ECS, based on their limited survey conducted in the "PN line" [13,14]. Thereafter, Chinese scientists launched large-scale field surveys to study the air-sea CO_2 exchanging process in ECS [5,7,9,10,15,16]. After entering the 21st century, a series of achievements relating to the CO_2 sink/source in ECS have been obtained, including understanding of the seasonal variation patterns and controlling factors of carbon cycling in the Changjiang estuary and its adjacent region [17–21], the difference of seawater carbonate conditions within the Yellow Sea [12,22], the potential evolution trends in ECS under increasing anthropogenic activities and the relevant influence for air-sea CO_2 exchanging flux [7,15,23].

New insights into the air-sea CO_2 exchanging process obtained in the ECS are of important guiding significance for exploring carbon cycling in various continental shelf seas of the world. For example, a study conducted in ECS in the summer revealed that the reason some heterotrophic marginal seas could act as significant CO_2 sinks was because of high biological productivity and concurrent intensive seasonal stratification [8,24]. What is more, extrapolating from observations conducted in the ECS, Tusungai et al. (1999) proposed the concept of "continental shelf pump" to explain why the ECS could absorb atmospheric CO_2 at a very high rate (2.92 mol $C/m^2/yr^1$) and suggested the continental shelf pump would account for a net oceanic uptake of CO_2 in the flux of 1.0 Pg C/yr, if the whole global continental shelf could absorb atmospheric CO_2 at the rate they obtained in the ECS [14].

Much research has already proven that the air-sea CO_2 exchanging process and the CO_2 source/sink pattern of the ECS are affected significantly by terrestrial material [17,25], which enters into the ECS substantially through the discharge of Changjiang River. The Changjiang River (also known as the Yangtze River), the world's fourth largest river, empties into the northwest part of the ECS and brings abundant fresh water, sediment, nutrient and organic matter into the ECS shelf [26,27]. However, apart from terrestrial material, the ecological environment of the ECS is also regulated profoundly by geochemical dynamics from the open sea [28]. The Kuroshio Current, the boundary of subtropical gyre in the western Pacific Ocean, transports a massive amount of warm, saline water and nutrients (e.g., NO_3^-, PO_4^{3-} and SiO_3^{2-}) into the ECS shelf and may serve as a major nutrient source for primary production in the ECS shelf [29–31]. Numerical studies have already proven that the nearshore Kuroshio branch current could even reach as far as the nearshore area within the 50m-isobath near 30.5° N and has affected the coastal ecosystem profoundly [31]. What is more, the intrusion of Kuroshio and its related variations are considered an important inducement for algal blooms and hypoxia in nearshore region of the ECS [31,32].

Enormous efforts have been made to study the effects of the Kuroshio Current on potential CO_2 sequestration in the ECS, on the basis of multidisciplinary projects conducted in the sea surrounding Taiwan [16,33–35]. The latest study suggests that the northwardly flowing Kuroshio Current could transport about 6.5×10^{12} g of biologically mediated DIC annually into the ECS [34], which accounted for about 22% to 50% of the CO_2 uptake rate ($13\sim30 \times 10^{12}$ g C/yr) in the ECS [5]. It was estimated that this input of DIC would lead to an increase of DIC/TA and Revelle factor for 3% and 15.5%, respectively. Hence, the importing of the Kuroshio Current would exert a counteracting influence on the capacity of CO_2 absorbance in the ECS [34]. However, the DIC flux evaluated in the above-mentioned research was derived totally in the summertime, when the intrusion of the Kuroshio into the ECS was most intensive. Yet the temporal variability of Kuroshio in other seasons and the fluxes for other species of carbonate parameters, such as particulate organic carbon (POC), were not considered [34].

The main purpose of this study is, therefore, to investigate the variations of diverse carbonate parameters (e.g., pH, pCO_2, DIC and POC) and to assess the controlling effects of environmental factors on them in the mainstream of Kuroshio off eastern Taiwan. Moreover, we also determined the intrusion pattern of Kuroshio into the ECS shelf during spring time, when the intrusion of Kuroshio just began to appear [36], based on evidence from carbon chemistry and also estimated the transports of various carbonate parameters from the Kuroshio off eastern Taiwan into the ECS shelf during that time.

2. Materials and Methods

2.1. Study Area Description

The East China Sea (ECS, 23°00′–33°10′ N, 117°11′–131°00′ E) is a broad temperate continental marginal sea surrounded by Mainland China, Taiwan, South Korea, Kyushu and Ryukyu Islands, an area 66% of which is located on the flat continental shelf (Figure 1). It is one of the largest marginal seas located in the western Pacific and is an extremely dynamic sea that is influenced by various currents, such as the South China Sea (SCS) water passing through the Taiwan Strait (TS), the Yellow Sea (YS) water from the Yellow Sea Coastal Current (YSCC). The largest river of Asia, the Changjiang River, flows into the ECS with an annual average water discharge of about 940 km^3/yr [37]. Moreover, the East Asian monsoon generally regulates the seasonal variation of precipitation and temperature of the ECS.

The Kuroshio Current primarily originates in the northward bifurcation of the North Equatorial Current off the east coast of the Philippines [38]. It enters into the ECS through the channel in the south of the Ryukyu Islands chain [39]. Influenced by the steep ECS continental slope, the mainstream of Kuroshio generally runs along the 200 m isobaths at a velocity of about 0.7~1.4 m/s [40] until it approaches the shoaling northern end of the Okinawa Trough, where it leaves from the shelf and turns east-southeastward. Finally, the mainstream of Kuroshio leaves from the continental margin around 129° E, 30.5° N and flows into the Pacific Ocean again through the Tokara Strait [41]. More importantly, model results indicated that there is a Kuroshio Bottom Branch Current to the northeast of Taiwan (KBBCNT), which upwells northwestward gradually from 300 m to 60 m in the region northeast of Taiwan, then turns northeast in the region around 27.5° N, 122° E and finally reaches 31° N off the Changjiang estuary following about 60 m isobaths, conveying saline, nutrient-rich Kuroshio Subsurface Water into the ECS shelf and even the Changjiang estuary [39].

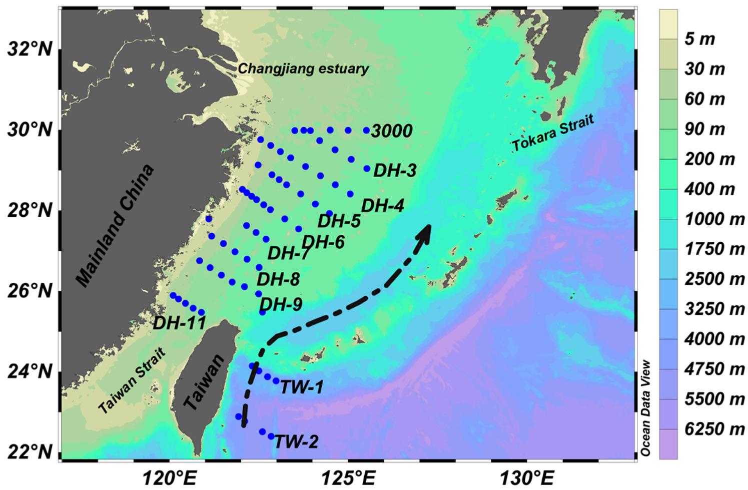

Figure 1. Study area and station location in our study. The black dash-dot line was the schematic diagram of the mainstream of Kuroshio Current.

2.2. Sampling and Analytical Methods

Field investigation was carried out in the continental shelf of the ECS and the eastern region of Taiwan on the R/V *Kexue I* from 18 May to 13 June 2014. A total of 55 investigation stations scattered evenly on the continental shelf of ECS and 8 stations located in the eastern of Taiwan, where the mainstream of Kuroshio flowed through (Figure 1). At each station, the recommended standard operating procedures described by Dickson et al. (2007) [42] and the methods of Chou et al. (2009a, 2009b) [7,8], Qu et al. (2017) and Zhai et al. (2014) [12,43] were adopted during the sampling and analytical processes. Generally, discrete seawater was sampled at seven to thirteen depths, with intervals of 10–500 m, using a rosette sampler with 10-liter Niskin sampling bottles, according to the bottom depth of each station. In the ECS, the sampling layers were 2 m (the surface layer), 10 m, 20 m, 30 m, 50m, 75 m, 100 m and 2 m above the seafloor (the bottom layer), while in eastern Taiwan, the sampling layers were 5 m (the surface layer), 30 m, 50 m, 75 m, 100 m, 150 m, 200 m, 300 m, 500 m, 800 m, 1000 m, 1500 m and 2000 m (the bottom layer).

The temperature (°C) and salinity (PSU) were recorded at each layer by a conductivity-temperature-depth (CTD) system (SBE-911 plus, Sea-Bird Electronics Inc., USA). The pH (the total hydrogen ion concentration scale) was measured on board at 25 ± 0.1 °C using a Orion Star™ and Star Plus meter (Thermo Electron, USA) with an Orion® Ross combination electrode (Thermo Fisher Scientific, USA), which was calibrated by buffers (2-amino-2-hydroxymethyl-1,3-propanediol (Tris) and 2-aminopyridine) prepared at a salinity of 35 [42]. The precision of the pH determination in this study was better than ±0.005 pH units [7,8] and the overall uncertainty was ±0.01 [43]. TA was measured using the method of Gran titration by way of an automatic potentiometric titrator (798 MPT Titrino, Metrohm, Switzerland), with a precision of 0.1–0.3% (±2 to ±6 μmol·kg^{-1}). Certified reference material from Prof. Dickson was used for calibration and quality control in the TA measurements [42]. The determination of total chlorophyll a (Chl *a*) concentration was conducted using a Turner Designs Model 10 fluorometer [44]. Partial pressure of CO_2 (pCO_2), Revelle Factor (RF) and carbonate saturation state (Ω_{Ca}) were calculated from TA and pH by the CO2SYS program of Lewis and Wallace (1998) [45], adopting the carbonate dissociation constants proposed by Mehrbach et al. (1973) [46], which was refitted by Dickson and Millero (1987) [47]. What is more, the pH scale in our calculation process was adopted as the seawater scale. The value of K_S, the dissociation constant for $HSO4^-$, was taken from Dickson (1990a) [48] and the value of K_B (for boric acid) was taken from Dickson (1990b) [49]. The measurement of dissolved oxygen (DO) concentration was performed aboard using the Winkler titration method with a precision of 7×10^{-5} mg/L [50]. Particulate organic carbon (POC) in filtered particulate matter was determined with a C/N analyzer (Elementar, vario EL cube, German) after inorganic carbonate was removed with a precision of ±0.3 μmol/L [51].

3. Results

3.1. Hydrographic Characteristics and Water Types Classification

The spatial distributions of the hydrographic parameter (temperature, salinity and density (ρ)) in the surface and bottom water of the ECS shelf and the eastern Taiwan are presented in Figure 2. In the surface layer, low temperature (<22.0 °C), low salinity (<30.0 PSU) and low density (<20.5 kg/m^3) water is confined to the nearshore region of the ECS (depth < 50 m). This kind of water is affected primarily by the Changjiang Diluted Water (CDW), which is created by the abundant freshwater discharged by Changjiang. The coverage of CDW could represent the impact strength of terrigenous input, to some extent. With increasing distance from the coastline, high temperature (>24.0 °C), high salinity (>33.0 PSU) and high density (>22.5 kg/m^3) began to appear in the offshore shelf of the ECS (50 m < depth < 200 m) and eastern Taiwan (500 m < depth < 5000 m) (Figure 2). In the bottom layer, however, the nearshore area was provided with the highest temperature but the lowest salinity and density and the offshore shelf of the ECS had relatively higher temperature salinity and density. Bottom seawater in eastern Taiwan possessed the lowest temperature (0< T< 7 °C), highest salinity (about 34.0 PSU) and highest density (about 27 kg/m^3) in our study area.

These above-mentioned variations of hydrographic parameters were closely related with the complicated circulation system of our studied region, which was basically composed of the Changjiang Diluted Water (CDW), the ECS Coastal Water (ECSCW), the Taiwan Warm Current (TWC) and the Kuroshio Current (KC) [52]. Based on the dataset of potential temperature (θ), salinity and potential density anomaly (σ0) we obtained, the water of the ECS and adjacent eastern Taiwan were categorized into seven water types (Figure 3 and Tables 1 and 2). First of all, waters in the ECS were simply classified as the ECS Coastal Water (ECSCW), the Taiwan Warm Current (TWC) and the Shelf Mixed Water (SMW). The ECSCW usually possessed the lowest temperature (18.87 °C < T < 23.88 °C) and salinity (S ≤ 31) among the seven water masses because it was strongly affected by riverine fresh water from Changjiang. The TWC originated from the subtropics water and flowed into the southwest of the ECS through the Taiwan Strait. This water generally shared the same salinity scope (31.30 < S < 34.50) with the SMW but it was warmer than the SMW by about 5 °C on average (Figure 3 and Table 1). Waters off the eastern Taiwan were divided into four parts, including the Kuroshio Surface Water (KSW, water depth 0~100 m, similarly hereinafter) with the highest temperature and high salinity (averaged temperature and salinity was 25.68 °C and 34.62 respectively, similarly hereinafter), the Kuroshio Subsurface Water (KSSW, 100~300 m) with relatively lower temperatures and the highest salinity (19.12 °C and 34.75), the Kuroshio Intermediate Water (KIW, 400~800 m) with much lower temperatures and the lowest salinity (7.65 °C and 34.33) and the Kuroshio Deep Water (KDW, 1000~2000 m) with the lowest temperature and low salinity (2.86 °C and 34.53).

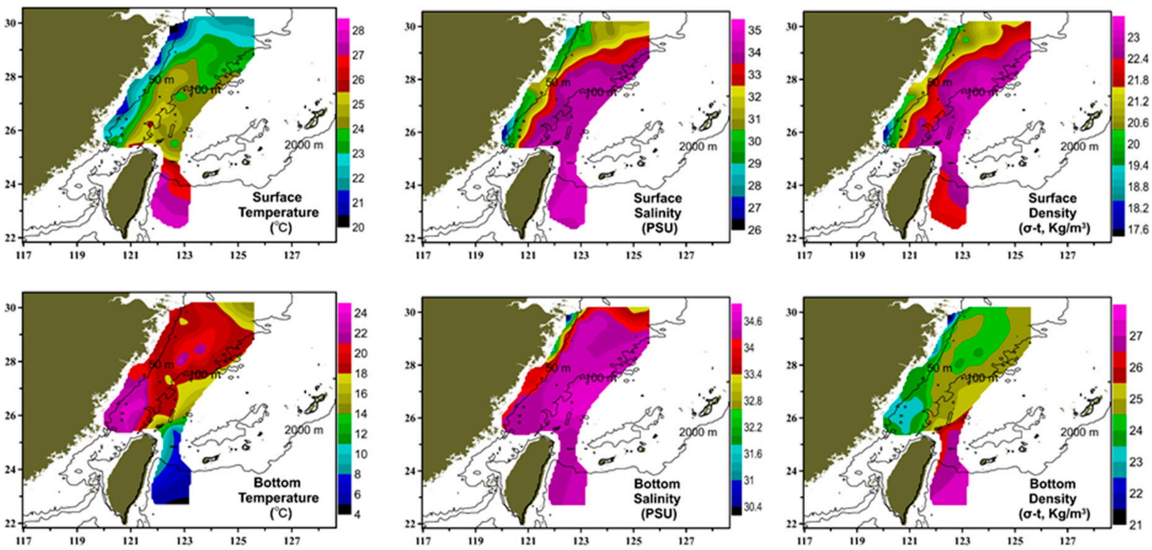

Figure 2. Spatial distributions of the hydrographic parameter (temperature (°C), salinity and density (kg/m^3) in the surface and bottom layer of the East China Sea (ECS) and eastern Taiwan.

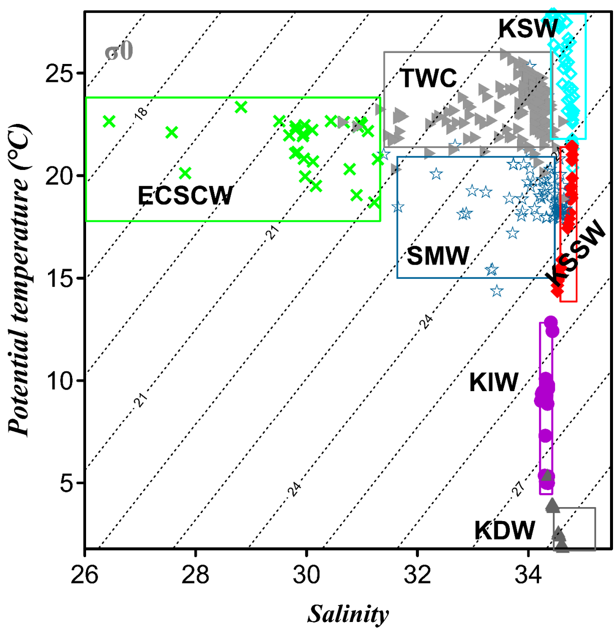

Figure 3. A plot of potential temperature (θ) and salinity of seawater at all stations in ECS shelf and eastern Taiwan. The dash-dot lines denote the isopycnals of potential density anomaly (σ0). The colorful rectangles represents different water masses, which include the ECS coastal water (ECSCW), Taiwan Warm Current (TWC), Shelf Mixed Water (SMW), Kuroshio Surface Water (KSW), Kuroshio Subsurface Water (KSSW), Kuroshio Intermediate Water (KIW) and Kuroshio Deep Water (KDW). The definitions of the water masses were based on Chen (2009), Chen and Wang (2006), Ichikawa and Chaen (2000), Qi et al. (2014) [53–56].

Table 1. Temperature and salinity variations in the various water types.

Water types	Temperature (°C)	Salinity (PSU)
ECSCW	18.87 < T < 23.88	26.34 < S < 31.20
TWC	21.69 < T < 25.83	31.33 < S < 34.28
SMW	16.25 < T < 21.02	31.40 < S < 34.49
KSW	20.39 < T < 27.89	34.34 < S < 34.82
KSSW	14.35 < T < 21.45	34.52 < S < 34.79
KIW	4.99 < T < 12.83	34.23 < S < 34.43
KDW	1.89 < T < 5.40	34.35 < S < 34.62

3.2. Profiles of Hydrological and Carbonate Parameters in Mainstream of Kuroshio off Eastern Taiwan

The continental margin off eastern Taiwan is the mainstream of the Kuroshio Current where it develops and intensifies to a strong western boundary current after leaving its source area east of Luzon Island. Due to the intensive island-continent collision, the seafloor topography in eastern Taiwan usually drops abruptly from the nearshore to more than 2000 m at a distance of only 40 to 50 km. Consequently, the concentration gradients of carbonate species across the mainstream of Kuroshio Current might be significantly. In the following paragraphs, we would present the vertical profiles of DIC (μmol/kg), pH@25 °C, DIC/TAlk, DO (mg/L), POC (μmol/L) and the calculated pCO$_2$ (μatm) and Revelle Factor observed in the two transects of TW-1 and TW-2 (Figure 1). Together with the typical features of temperature (°C), salinity (PSU) and density (kg/m^3), the carbonate characteristics in different parts of Kuroshio Current would be demonstrated.

As for the hydrological parameters, temperature, density and salinity ranged 1.88~27.95 °C, 22.03~27.68 kg/m^3 and 34.24~34.83, respectively (Figures 4a–c and 5a–c). Temperature decreased gradually with the increasing of water depth when it was shallower than 1000 m and basically held steady as the water was deeper than 1000 m. The density shown opposite vertical distribution pattern with temperature, which increased as the depth increased and also remained stable in water deeper than 1000 m. Salinity initially displayed an increasing trend in the above 150 m and then decreased in water column of 150~500 m. Furthermore, salinity turned to increase again when the water was deeper than 500 m.

Figures 4d and 5d presented the profile of pH@25 °C (pH values normalized to 25 °C) measured at transect TW-1 and TW-2. Vertical distribution of pH@25 °C basically possessed similar pattern with that of temperature, namely the upper layer had relative high pH values (7.80~8.20) while the pH values in under layer were relative low (7.50~7.80) (Figures 4d and 5d). In the case of DIC, DIC/TAlk, pCO$_2$ and Revelle factor, similar vertical distribution structures were found in eastern Taiwan. In particular, DIC increased gradually from a consistent surface value of about 1860 μmol/kg to nearly 2400 μmol/kg at the depth of 2000 m (Figures 4e and 5e). Thus, the increase of DIC from the surface to 2000 m was accompanied by a decrease of temperature and an increase of density. Our DIC results were comparable to those previous investigations conducted in this area [34,57]. The ratio of DIC/TAlk, which could serve as an indicator for pCO$_2$, varied from 0.81 in the surface seawater to 0.99 in the bottom water (Figures 4f and 5f). The relatively consistent DIC/TAlk below 500 m (0.97~1.00) indicated the stable inorganic carbonate condition for deep water column off eastern Taiwan. The calculated pCO$_2$ (μatm) and Revelle Factor also displayed an increasing trend from the surface seawater to the bottom water. As for the pCO$_2$, it was less than the atmospheric CO$_2$ value (402 μatm) in the upper 100 m water column (Figures 4g and 5g), accompanied by a relatively low Revelle Factor (about 8.0~9.0) (Figures 4h and 5h). The difference of pCO$_2$ between the atmosphere and the surface seawater was usually employed to calculate the air-sea CO$_2$ exchange flux. It ranged from −182 μatm to −153 μatm with an average of −121 μatm in the surface seawater of stations off eastern Taiwan (Figures 4g and 5g).

Based on Figures 4i and 5i, the DO averaged about 6.5 mg/L at the surface water and then decreased rapidly to approximately 4.1 mg/L at 500 m. In the water column of 800~1000 m, there was an oxygen minimum zone (OMZ) with DO contents of 2.38~2.81 mg/L. This kind of DO profile in our study was consistent with those observed in the Atlantic and Pacific Ocean [58–60], implying the seawater off eastern Taiwan was equipped with specific characteristics of the open sea. Concentrations of POC in eastern Taiwan generally shared similar vertical profiles, which basically enriched the surface and upper column of seawater and remained at a relatively low level in the under layer water (Figures 4j and 5j). Values of POC measured in this article were comparable to those reported in the northeastern Taiwan [61].

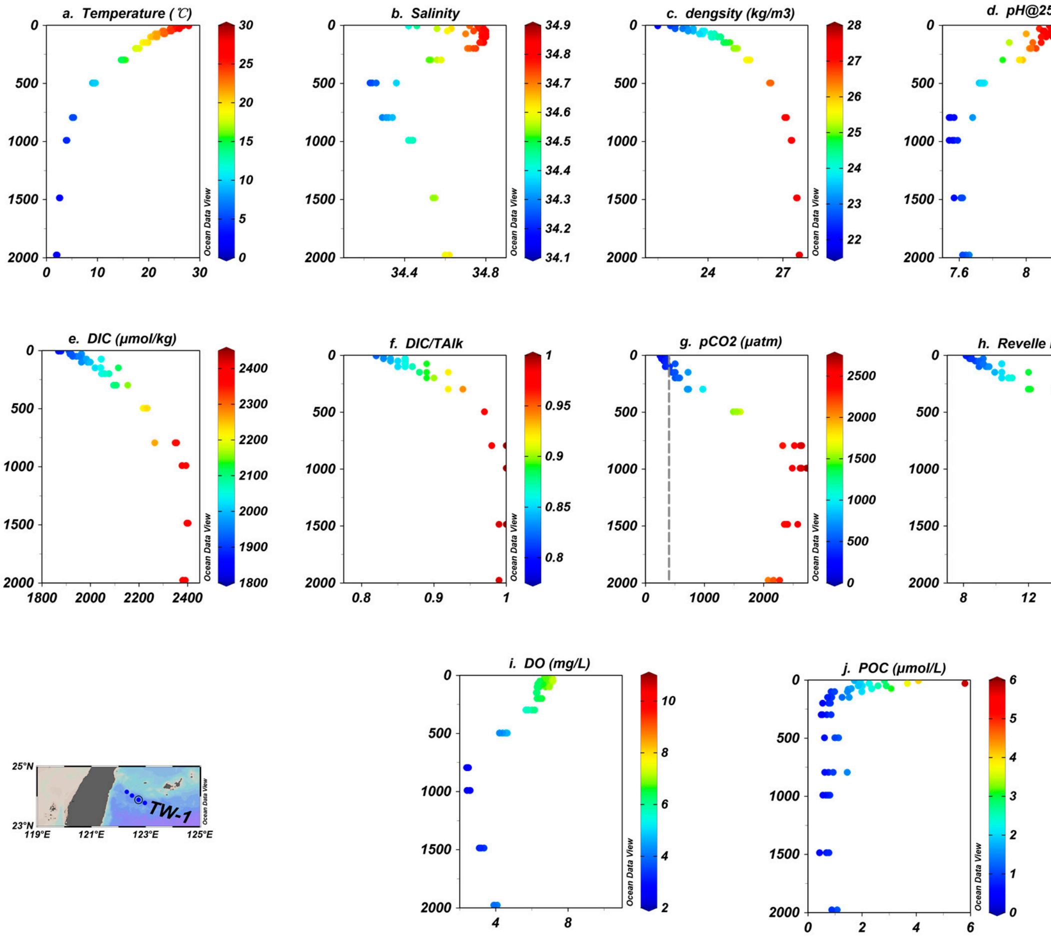

Figure 4. Vertical distributions of temperature (°C), salinity, density (kg/m^3), DIC (µmol/kg), pH@25°C, DIC/TAlk, DO (mg/L), POC (µmol/L) and the calculated pCO$_2$ (µatm) and Revelle Factor along transect TW-1, eastern Taiwan. The gray dashed line in vertical distributions of pCO$_2$ indicated the atmospheric CO$_2$ value in May 2014 (402 µatm, https://www.co2.earth/monthly-co2).

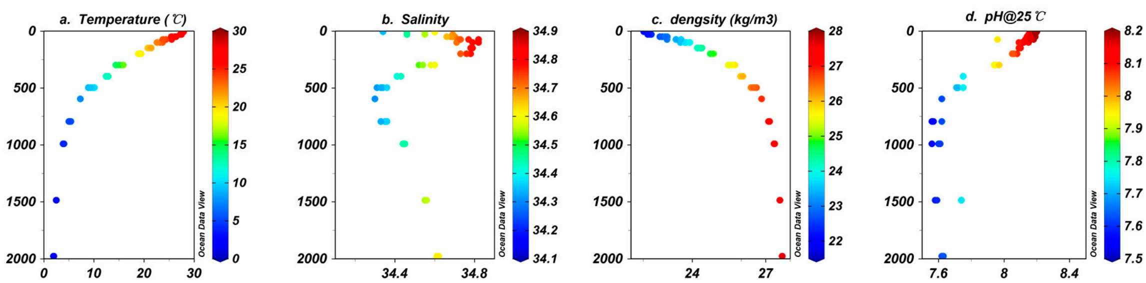

Figure 5. *Cont.*

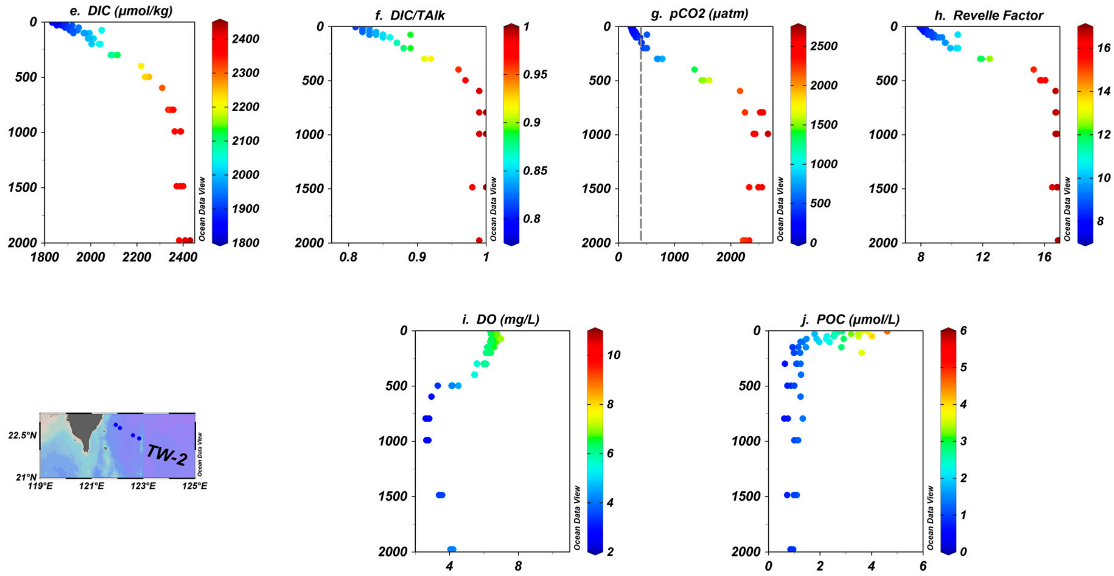

Figure 5. Vertical distributions of temperature (°C), salinity, density (kg/m^3), DIC (μmol/kg), pH@25 °C, DIC/TAlk, DO (mg/L), POC (μmol/L) and the calculated pCO_2 (μatm) and Revelle Factor along transect TW-2, eastern Taiwan. The gray dashed line in vertical distributions of pCO_2 indicated the atmospheric CO_2 value in May 2014 (402 μatm, https://www.co2.earth/monthly-co2).

3.3. Summary for Carbonate Chemistry in the Mainstream of Kuroshio

According to the classification of water types conducted in the mainstream of Kuroshio (please see details in Section 3.1 and Figure 3), we summarized the average contents of various carbonate species for KSW, KSSW, KIW and KDW in Table 3. The results briefly indicated that the KSW had the highest biologically-related parameters such as pH, POC and Ω_{Ca} in the four water masses but the lowest DIC, pCO_2 and RF. In particular, the average pCO_2 value of this water mass (312 μatm) was lower than the level of atmospheric CO_2 (402 μatm, data source: https://www.co2.earth/monthly-co2), which demonstrated the KSW could serve as an atmospheric sink during our investigating period. On account of the fact that the KSW was the only water located above the eutrophic layer, it could reasonably be deduced that biological activity was probably the important controlling factors for carbonate system in the KSW. The KIW and KDW possessed quite low contents of pH and Ω_{Ca}, yet high contents of DIC and pCO_2. These results suggested the KIW and KDW stored abundant inorganic carbon and seawater in these two water masses was quite acidic with respect to the surface water column. As for the KSSW, which could affect the ECS shelf ecosystem through physical processes such as upwelling, vertical mixing and cyclonic mesoscale, moderate range of carbonate parameters were found in this water masses. For the sake of exploring internal influence of Kuroshio on the CO_2 source/sink of adjacent continental shelf, the relationships between carbonate parameters and related controlling factors and the cross-shelf transport of various carbonate species were presented in the following paragraphs.

Table 2. Contents of hydrological and ecological-related parameters (mean ± standard deviation) in different water masses of mainstream of Kuroshio off eastern Taiwan (KSW, KSSW, KIW, KDW).

	T (°C)	Salinity	ρ (kg/m^3)	Chl *a* (μg/L)	DO (mg/L)
KSW	27.74 ± 2.26	34.68 ± 0.13	23.16 ± 0.76	025 ± 0.25	6.7 ± 0.2
KSSW	17.92 ± 2.29	34.69 ± 0.10	25.04 ± 0.49	0.04 ± 0.03	6.2 ± 0.3
KIW	8.01 ± 2.63	34.33 ± 0.05	26.71 ± 0.39	not detected	3.6 ± 1.0
KDW	2.99 ± 0.99	34.52 ± 0.08	27.50 ± 0.16	not detected	3.3 ± 0.6

Note: The definitions of water masses were conducted in Section 3.1.

Table 3. Contents of various carbonate species (mean ± standard deviation) in different water masses of mainstream of Kuroshio off eastern Taiwan (KSW, KSSW, KIW and KDW).

	KSW	KSSW	KIW	KDW
pH@25 °C	8.141 ± 0.05	8.013 ± 0.069	7.692 ± 0.135	7.606 ± 0.043
DIC (μmol/kg)	1930 ± 51	2064 ± 46	2274 ± 63	2389 ± 16
DIC/TAlk	0.84 ± 0.02	0.90 ± 0.02	0.98 ± 0.02	0.99 ± 0.01
pCO$_2$ (μatm)	312 ± 68	597 ± 156	1869 ± 568	2401 ± 216
RF	8.74 ± 0.59	11.07 ± 1.17	15.98 ± 1.10	16.80 ± 0.10
POC (μmol/L)	2.5 ± 1.0	1.1 ± 0.7	0.9 ± 0.3	0.9 ± 0.2
Ω_{Ca}	6.1 ± 0.7	4.0 ± 0.7	1.6 ± 0.5	1.1 ± 0.1

Note: The definitions of water masses were conducted in Section 3.1.

4. Discussion

4.1. Relationships between Carbonate Parameters and Environmental Factors in Kuroshio

The relationships between pCO$_2$, DIC and environmental parameters (e.g., temperature, salinity, DO) will be discussed in this section. To be specific, there were strong negative correlations between pCO$_2$ and temperature in the KSW ($r = -0.707$, $p < 0.01$, $n = 41$) and the KSSW ($r = -0.861$, $p < 0.01$, $n = 21$) (Figure 6). Normally, temperature was supposed to show a positive correlation with pCO$_2$ in the perspective of thermodynamic [62,63]. However, external import of CO$_2$-rich cold water and biological activity were considered to be the most two important causations for this negative correlation [11]. Similar negative correlations were also observed in a cold-core cyclonic eddy in Hawaiian Islands [64], the offshore region of south Yellow Sea in the winter and summer [65] and the inner and middle shelf of ECS in winter [9].

In order to explore the internal controlling effects of environmental factors in KSW, we provided that a water with a constant TAlk of 2291 μmol/kg (the average TAlk for KSW) is in equilibrium with an atmospheric pCO$_2$ of 402 μatm (the average of the atmospheric pCO$_2$ measurements off eastern Taiwan). The temperature dependence of DIC in this hypothetical water parcel can be calculated as −7.6 μmol kg/°C (blue line in Figure 7a). This value was less than the observed slope of the DIC *vs.* temperature relationship (slope = −17.3 μmol kg/°C, red line in Figure 7a). What is more, we found a negative correlation between measured DIC and DO ($r = -0.326$, $p < 0.05$, $n = 41$) and a positive correlation between DIC difference (DIC $_{calculated}$ minus DIC $_{measured}$) and DO contents in KSW ($r = 0.423$, $p < 0.01$, $n = 39$) (Figure 7b). Therefore, this kind of discrepancy between calculated DIC (blue symbols in Figure 7a) and measured DIC (red symbols in Figure 7a) should be attributed to an additional DIC "sequestration" process which generally derived from phytoplankton photosynthesis. Namely, biological activity actually affected the carbonate system of KSW profoundly. However, there was no significant correlation between DIC and Chl *a*. The reason for the deviation in Chl *a* content from primary production was most likely the result of grazing pressure exerted by zooplankton [44].

We also compared the measured DIC and calculated DIC in the KSSW, based on the same assumptions carried out in KSW. The results demonstrated that the interrelation between DIC $_{calculated}$ and DIC $_{measured}$ showed two opposing trends: DIC $_{measured}$ was higher than DIC $_{calculated}$ for water with temperature <19.4 °C, whereas DIC $_{measured}$ was lower than the DIC $_{calculated}$ for water with temperature >19.4 °C (Figure 8a). The positive differences between DIC $_{measured}$ and DIC $_{calculated}$ when temperature >19.4 °C was similar with the situation of KSW, indicating the regulating effects of biological activity on DIC variation still occurred in the relative warmer layer of KSSW. However, the negative difference between DIC $_{measured}$ and DIC $_{calculated}$ when temperature <19.4 °C was very likely related to the external transport of DIC-enriched water, which was probably from the South China Sea (SCS). A study conducted in the Luzon Strait and eastern Taiwan demonstrated that the SCS subsurface water that was rich in biological fixed carbon could significantly modify the carbon chemistry of the subsurface water of the Kuroshio Current in regions off southeast Taiwan [33,35].

Accordingly, we plotted the DIC *vs.* salinity and DIC *vs.* density in KSSW and found that the DIC in KSSW was negatively related to salinity ($r = -0.811$, $p < 0.01$, $n = 41$) and positively related to density ($r = 0.838$, $p < 0.01$, $n = 41$) (Figure 8b). These findings suggested that DIC was likely to be enriched in the saline and dense endmember of KSSW, which was probably derived from the SCS. Nevertheless, the potential influence of external DIC transportation on the carbon chemistry of KSSW was far from resolved and further study was needed.

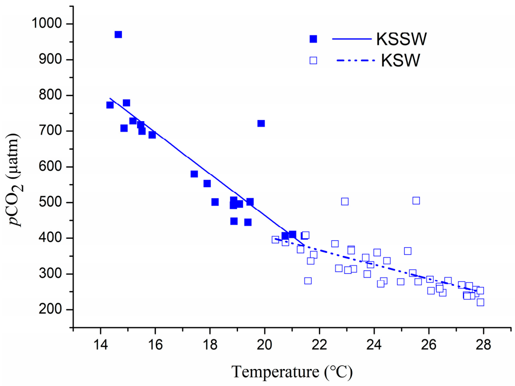

Figure 6. Diagrams of pCO_2 vs. temperature for the Kuroshio Surface Water (KSW) (blue hollow squares) and the Kuroshio Subsurface Water (KSSW) (blue filled squares) off eastern Taiwan.

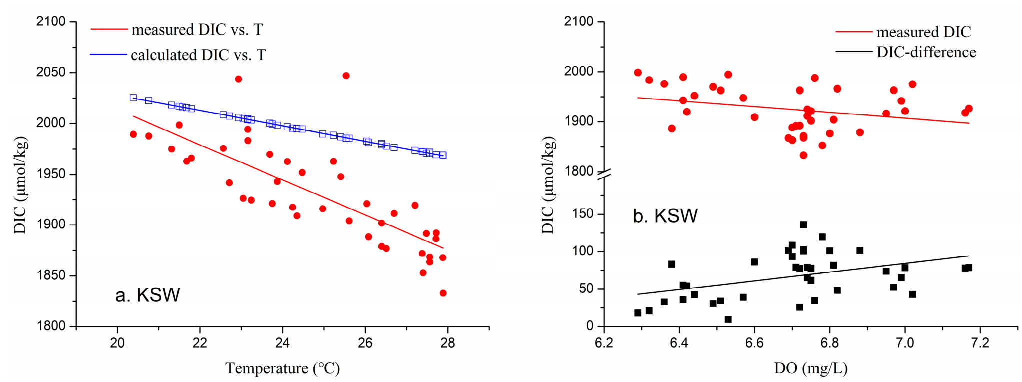

Figure 7. (**a**) Diagrams of measured and calculated DIC vs. temperature for the Kuroshio Surface Water (KSW). (**b**) Diagrams of measured DIC and DIC difference (calculated DIC minus measured DIC) *vs*. dissolved oxygen in the KSW.

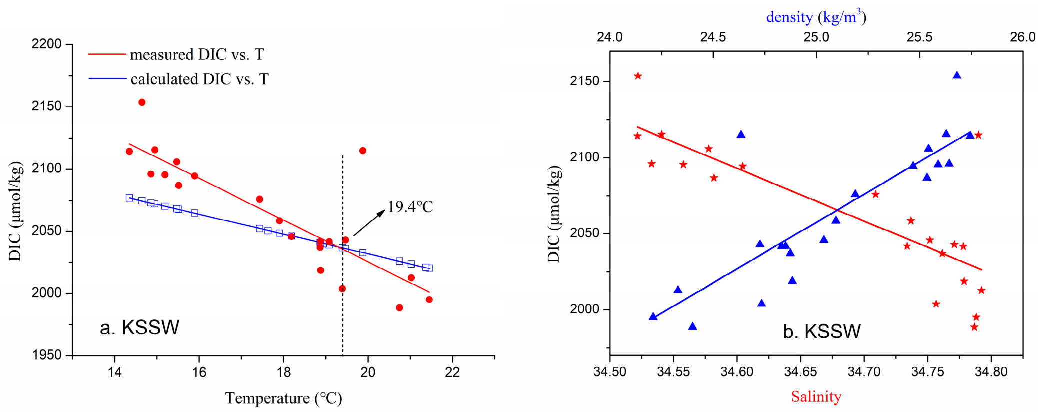

Figure 8. (**a**) Diagrams of measured and calculated DIC vs. Temperature for the Kuroshio Subsurface Water (KSSW). (**b**) Plots of DIC vs. salinity and density in the KSSW.

4.2. Intrusion of Kuroshio off Eastern Taiwan into the ECS Shelf: Evidence from Carbon Chemistry Parameters

The distribution patterns of the hydrographic data and the carbonate parameters in transect DH-9, which is the nearest transect to northeast of Taiwan, are shown in Figure 9. The temperature, salinity, density in transect DH-9 showed typical slanted isoclines toward the west/shelf (Figure 6a–c). In detail, a mass of water with low temperature (T < 20.0 °C), high salinity (S > 36.5) and density (ρ > 24.5 kg/m^3) occupied the bottom layer of this transect (Figure 9a–c), implying the upwelling of the northwardly flowing Kuroshio waters. Correspondingly, we found that this water mass in transect DH-9 (marked in Figure 9 by an arrow symbol) possessed a relatively high concentration of DIC, DIC/TAlk, pCO$_2$ and Revelle Factor (RF) but low pH and Ω_{Ca} (Figure 9d–i). In other words, the upwelling of Kuroshio water off northeastern Taiwan could not only transport cold, saline and dense water mass into the southern ECS shelf but also could convey water mass with a high content of DIC, DIC/TAlk and RF, low pH and Ω_{Ca} into the southern ECS shelf.

It had already been found that the cold, nutrient-rich KSSW intruded into the southern ECS shelf and was a major nutrient source to maintain high productivity [30,35]. However, the influence scope of KSSW on ECS is still in debate. It had been reported that the KSSW in eastern Taiwan could intrude into the ECS as far as its nearshore region by a Nearshore Kuroshio Branch Current (NKBC), which linked the nutrient-rich KSSW with the ECS shelf [31,39,66]. In this paper, we supplemented the vertical profiles of temperature, salinity, density, DIC, DIC/TAlk, pH@25 °C, pCO$_2$, Revelle Factor and Ω_{Ca} in transect DH-5, which was located near the Changjiang estuary, in order to verify whether the water mass with a high content of DIC observed in transect DH-9 could appeared in transect DH-5 (Figure 10). Our findings demonstrated that, in the outer endmember of transect DH-5, water mass that had a relatively high concentration of DIC, DIC/TAlk, pCO$_2$ and Revelle Factor (RF), low pH and Ω_{Ca} was also observed just like the situation in transect DH-9 (Figure 10d–i). Consequently, it could be inferred that the Kuroshio Current off eastern Taiwan could exactly intrude into the ECS shelf as far as 27.9° E, 125.5° N (the outer endmember of transect DH-5), basing on the evidence of carbon chemistry.

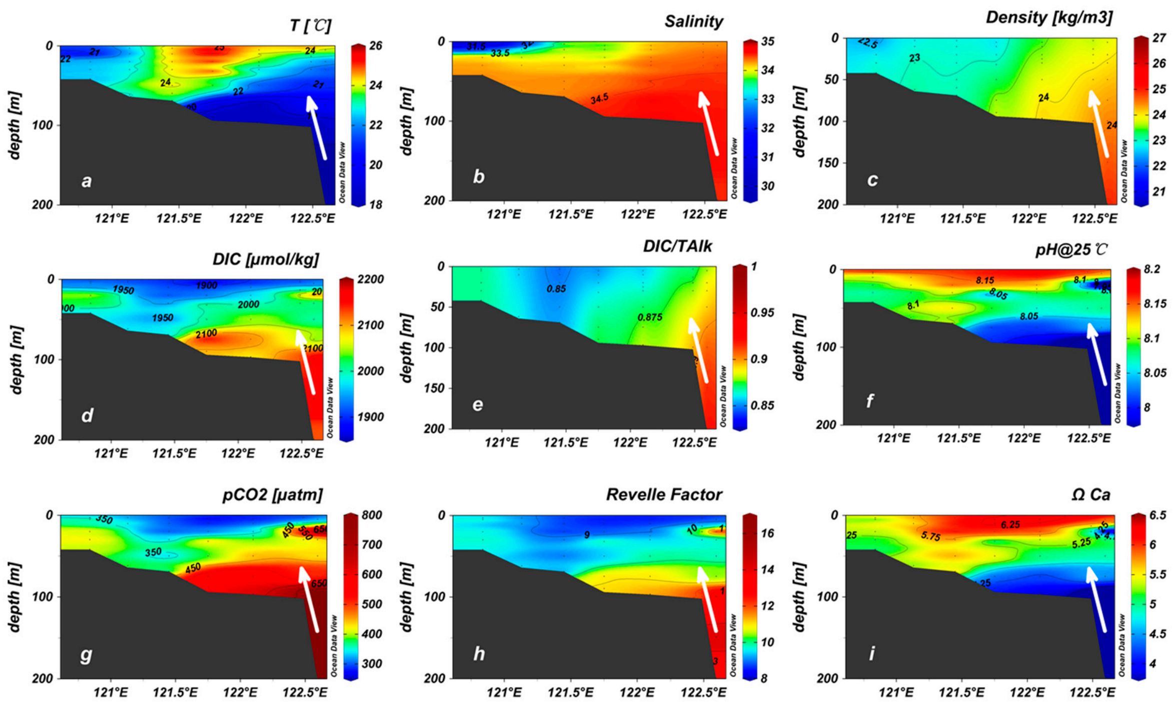

Figure 9. Vertical profiles of (**a**) temperature, (**b**) salinity, (**c**) density, (**d**) DIC, (**e**) DIC/TAlk, (**f**) pH@25 °C, (**g**) pCO$_2$, (**h**) Revelle Factor, (**i**) Ω_{Ca} in transect DH-9. The white arrow indicated the upwelling of Kuroshio Current in the northeastern Taiwan.

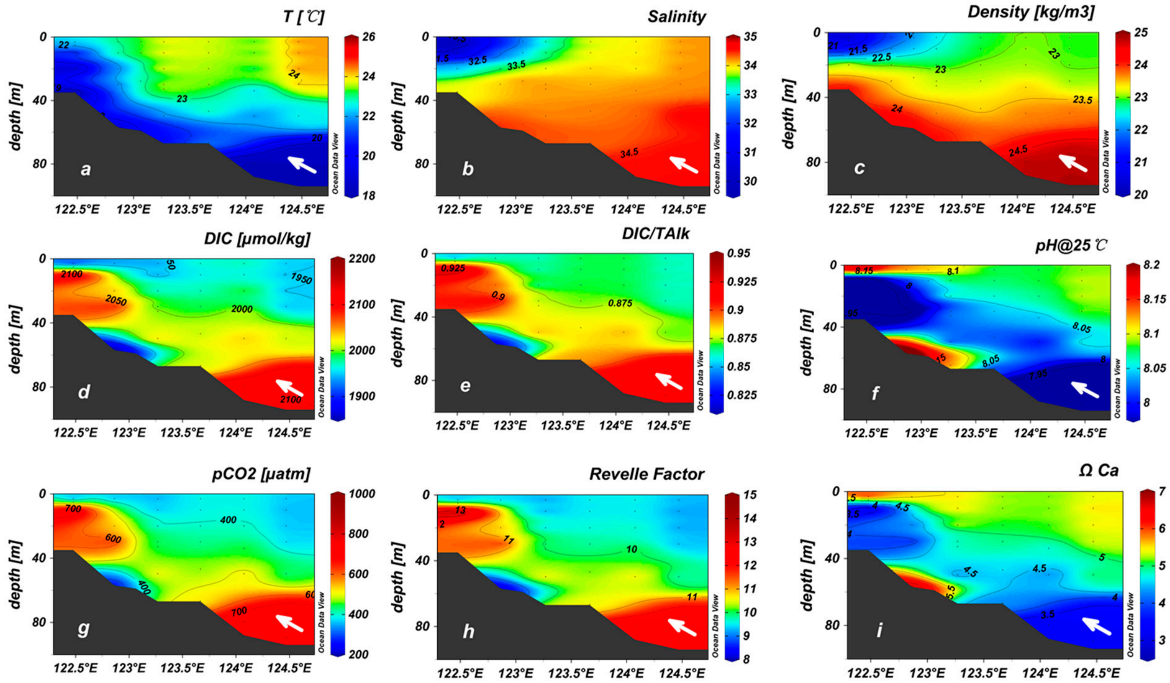

Figure 10. Vertical profiles of (**a**) temperature, (**b**) salinity, (**c**) density, (**d**) DIC, (**e**) DIC/TAlk, (**f**) pH@25 °C, (**g**) pCO_2, (**h**) Revelle Factor, (**i**) Ω_{Ca} in transect DH-5.

4.3. Estimates of Carbon Transport from Kuroshio into the ECS Shelf

As discussed in Section 4.2, the Kuroshio upwelled waters were characterized by high DIC/TA ratio and Revelle factor. As these upwelled waters flowed northwardly and entered into the ECS shelf finally, they would profoundly change the carbonate properties and CO_2 absorption capacity in the ECS, which was probably the most important oceanic atmospheric CO_2 sink for China [67]. In the following paragraphs, we tried to evaluate the impact of the intruded Kuroshio water to the DIC pool in the ECS shelf. The water fluxes budget for the ECS in rainy season (May to October), which was evaluated by Zuo et al. (2016) based upon a simple box model about water and salt, was adopted in the estimation of DIC transport [68] (Figure 11). This water flux budget was in good agreement with the latest research results [39,69]. As for the estimation of carbon transport, the following formulation was adopted: $F = C \times Q$, where F represented the transport flux (Tg C, 1 Tg = 10^{12} g), C was the average concentration for various carbon parameters (μmol/L) and Q stood for the water flux (Sv, 1 Sv = 10^6 m^3/s).

Results of all these transport fluxes are summarized in Table 4. As a result, the KSW, KSSW and KIW could convey DIC into the ECS shelf with a flux of 285, 305 and 112 Tg C/half year (1 Tg = 10^{12} g), respectively (Table 4). And the relevant flux of POC for KSW, KSSW and KIW was 0.16, 2.93 and 0.04 Tg C/half year, respectively (Table 4). The results indicated that the total influx of DIC (702 Tg C/half year) from the Kuroshio was much larger than the CO_2 uptake rate (13~30 Tg C/yr) in ECS through air-sea CO_2 exchanging process [5]. This great difference should be attributed to the fact that some of the Kuroshio water might only stay a short time in the ECS, thus will not remain in the ECS for a long time. In particular, since carbonate species transport fluxes estimated in the present study were derived basically from their depth profiles in spring time, seasonal variability and related changes in upwelling that may vary obviously were not considered.

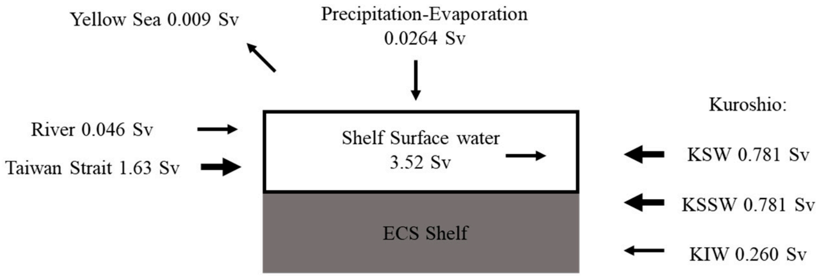

Figure 11. Schematic diagram of the water budgets (Sv) for the ECS Shelf in rainy season (May–October). 1 Sv = 10^6 m^3/s. Data was derived from the summary conducted by Zuo et al. (2016) [68].

Table 4. Water fluxes and estimates of various carbonate species transport from Kuroshio into the ECS shelf.

	Water Flux	DIC Input (10^{12} g)	POC Input (10^{12} g)
KSW	0.781	285	0.37
KSSW	0.781	305	0.16
KIW	0.260	112	0.04
total	1.82	702	0.57

5. Conclusions

The Kuroshio Current, as the famous western boundary of the subtropical gyre in the North Pacific Ocean, transports an abundant amount of warm saline water and nutrients (e.g., nitrate, phosphate, silicate) into the ECS shelf and serves as a major nutrients source for primary production in the southern ECS. Moreover, the transport of excess dissolved inorganic carbon (DIC) could restrain the ability of CO_2 sequestration in marginal seas. In this study, comprehensive carbon chemistry data including pH@25 °C, dissolved inorganic carbon (DIC), ratio of dissolved inorganic carbon and total alkalinity (DIC/TAlk), partial pressure of CO_2 (pCO_2), particulate organic carbon (POC), Revelle Factor (RF) and carbonate saturation state (Ω_{Ca}) were measured in the mainstream of Kuroshio off eastern Taiwan in May 2014.

The results indicated that the vertical variations of these carbonate species were closely related the characteristics of various water masses in the Kuroshio Current. Kuroshio Surface Water (KSW) had the highest biological-related parameters such as pH@25 °C, POC and Ω_{Ca} but the lowest DIC, pCO_2 and RF, which consistently demonstrated that this water could serve as an atmospheric CO_2 sink. However, low pH@25 °C, POC and Ω_{Ca} and high DIC, pCO_2 and RF were found in the Kuroshio Intermediate Water (KIW) and Kuroshio Deep Water (KDW). The Kuroshio Subsurface Water (KSSW), which is traditionally considered an important nutrient source for ECS shelf, possessed the moderate level of carbonate parameters.

Relationships interpretations among pCO_2, DIC, temperature and dissolved oxygen (DO) demonstrated phytoplankton photosynthesis played important controlling roles on DIC variation in KSW, whereas the DIC variation in KSSW was controlled not only by the above-mentioned biological activity but the external transport of DIC-enriched water from the South China Sea (SCS). In this article, we found the Kuroshio Current in eastern Taiwan could exactly intrude into the ECS shelf as far as 27.9° E, 125.5° N, basing on the evidence of carbon chemistry obtained in transects DH-9 and DH-5. This study also tried to evaluate the impact of the intruded Kuroshio water to the carbon pool in the ECS shelf. In general, the KSW, KSSW and KIW could convey DIC into the ECS shelf with flux of 285, 305 and 112 Tg C/half year (1 Tg = 10^{12} g), respectively. And the relevant flux of POC for KSW, KSSW and KIW was 0.16, 2.93 and 0.04 Tg C/half year, respectively. Although carbonate species estimated in this study were derived exclusively from the spring time and seasonal variability and possible changes in upwelling intensity that may vary obviously were not considered, the transportation of carbon from the Kuroshio to the ECS shelf might further exert a counteracting influence on the potential of atmospheric CO_2 absorption in the ECS, which needed intensive study in the future.

Supplementary Materials: The following are available online at http://www.mdpi.com/2071-1050/10/3/791/s1.

Acknowledgments: We are grateful to the captain and crew of R/V *Kexue I* for their shipboard operations and help during the filed investigation. Constructive comments from anonymous reviewers have greatly improved the quality of this manuscript. This study is supported by the Strategic Priority Research Program of the Chinese Academy of Sciences (No. XDA11020102) and the Joint Fund of Shandong Province and National Natural Science Foundation of China (No. U1406404).

Author Contributions: Baoxiao Qu, Jinming Song and Huamao Yuan conceived and designed the experiments; Baoxiao Qu and Huamao Yuan performed the experiments and analyzed the data; Xuegang Li and Ning Li contributed reagents/materials/analysis tools; Baoxiao Qu wrote the paper.

Conflicts of Interest: The authors declare no conflict of interest. The founding sponsors had no role in the design of the study; in the collection, analyses, or interpretation of data, in the writing of the manuscript and in the decision to publish the results.

References

1. Sabine, C.L.; Feely, R.A.; Gruber, N.; Key, R.M.; Lee, K.; Bullister, J.L.; Wanninkhof, R.; Wong, C.S.; Wallace, D.W.R.; Tilbrook, B.; et al. The oceanic sink for anthropogenic CO_2. *Science* **2004**, *305*, 367–371. [CrossRef] [PubMed]
2. Kempe, S.; Pegler, K. Sinks and sources of CO_2 in coastal seas—The North-Sea. *Tellus B* **1991**, *43*, 224–235. [CrossRef]
3. Thomas, H.; Bozec, Y.; Elkalay, K.; de Baar, H.J.W. Enhanced open ocean storage of CO_2 from shelf sea pumping. *Science* **2004**, *304*, 1005–1008. [CrossRef] [PubMed]
4. Walsh, J.J. Importance of continental margins in the marine biogeochemical cycling of carbon and nitrogen. *Nature* **1991**, *350*, 53–55. [CrossRef]
5. Wang, S.-L.; Chen, C.-T.A.; Hong, G.-H.; Chung, C.-S. Carbon dioxide and related parameters in the East China Sea. *Cont. Shelf. Res.* **2000**, *20*, 525–544. [CrossRef]
6. Chen, C.-T.A.; Wang, S.-L. Carbon, alkalinity and nutrient budgets on the East China Sea continental shelf. *J. Geophys. Res.* **1999**, *104*, 20675–20686. [CrossRef]
7. Chou, W.-C.; Gong, G.-C.; Sheu, D.D.; Hung, C.-C.; Tseng, T.-F. Surface distributions of carbon chemistry parameters in the East China Sea in summer 2007. *J. Geophys. Res.* **2009**, *114*, 1–12. [CrossRef]
8. Chou, W.-C.; Gong, G.-C.; Sheu, D.D.; Jan, S.; Hung, C.-C.; Chen, C.-C. Reconciling the paradox that the heterotrophic waters of the East China Sea shelf act as a significant CO_2 sink during the summertime: Evidence and implications. *Geophys. Res. Lett.* **2009**, *36*, 1–5. [CrossRef]
9. Chou, W.-C.; Gong, G.-C.; Tseng, C.-M.; Sheu, D.D.; Hung, C.-C.; Chang, L.-P.; Wang, L.-W. The carbonate system in the East China Sea in winter. *Mar. Chem.* **2011**, *123*, 44–55. [CrossRef]
10. Peng, T.-H.; Hung, J.-J.; Wanninkhof, R.; Millero, F.J. Carbon budget in the East China Sea in spring. *Tellus B* **1999**, *51*, 531–540. [CrossRef]
11. Qu, B.X.; Song, J.M.; Yuan, H.M.; Li, X.G.; Li, N. Air-sea CO_2 exchange process in the southern Yellow Sea in April of 2011 and June, July, October of 2012. *Cont. Shelf. Res.* **2014**, *80*, 8–19. [CrossRef]
12. Qu, B.X.; Song, J.M.; Yuan, H.M.; Li, X.G.; Li, N.; Duan, L.Q. Comparison of carbonate parameters and air-sea CO_2 flux in the southern Yellow Sea and East China Sea during spring and summer of 2011. *J. Oceanogr.* **2017**, *73*, 365–382. [CrossRef]
13. Tsunogai, S.; Watanabe, S.; Nakamura, J.; Ono, T.; Sato, T. A Preliminary study of carbon system in the East China Sea. *J. Oceanogr.* **1997**, *53*, 9–17. [CrossRef]
14. Tsunogai, S.; Watanabe, S.; Sato, T. Is there a "continental shelf pump" for the absorption of atmospheric CO_2? *Tellus B* **1999**, *51*, 701–712. [CrossRef]
15. Qu, B.; Song, J.; Li, X.; Yuan, H.; Li, N.; Ma, Q. $p$$CO_2$ distribution and CO_2 flux on the inner continental shelf of the East China Sea during summer 2011. *Chin. J. Oceanol. Limnol.* **2013**, *31*, 1088–1097. [CrossRef]
16. Wong, G.T.F.; Chao, S.-Y.; Li, Y.-H.; Shiah, F.-K. The Kuroshio edge exchange processes (KEEP) study—An introduction to hypotheses and highlights. *Cont. Shelf. Res.* **2000**, *20*, 335–347. [CrossRef]

17. Chen, C.-T.A.; Zhai, W.D.; Dai, M.H. Riverine input and air-sea CO_2 exchanges near the Changjiang (Yangtze River) Estuary: Status quo and implication on possible future changes in metabolic status. *Cont. Shelf. Res.* **2008**, *28*, 1476–1482. [CrossRef]
18. Gao, X.L.; Song, J.M.; Li, X.G.; Li, N.; Yuan, H.M. pCO$_2$ and carbon fluxes across sea-air interface in the Changjiang Estuary and Hangzhou Bay. *Chin. J. Oceanol. Limnol.* **2008**, *26*, 289–295. [CrossRef]
19. Li, X.G.; Song, J.M.; Yuan, H.M.; Li, N.; Duan, L.Q.; Qu, B.X. CO_2 flux and seasonal variability in the turbidity maximum zone and surrounding area in the Changjiang River estuary. *Chin. J. Oceanol. Limnol.* **2015**, *33*, 222–232. [CrossRef]
20. Guo, X.H.; Zhai, W.D.; Dai, M.H.; Zhang, C.; Bai, Y.; Xu, Y.; Li, Q.; Wang, G.Z. Air-sea CO_2 fluxes in the East China Sea based on multiple-year underway observations. *Biogeosciences* **2015**, *12*, 5495–5514. [CrossRef]
21. Song, J. *Biogeochemical Processes of Biogenic Elements in China Marginal Seas*; Springer: Berlin/Heidelberg, Germany, 2010.
22. Qu, B.X.; Song, J.M.; Yuan, H.M.; Li, X.G.; Li, N.; Duan, L.Q.; Chen, X.; Lu, X. Summer carbonate chemistry dynamics in the Southern Yellow Sea and the East China Sea: Regional variations and controls. *Cont. Shelf Res.* **2015**, *111*, 250–261. [CrossRef]
23. Lui, H.-K.; Chen, C.-T.A.; Lee, J.; Wang, S.-L.; Gong, G.-C.; Bai, Y.; He, X.Q. Acidifying intermediate water accelerates the acidification of seawater on shelves: An example of the East China Sea. *Cont. Shelf Res.* **2015**, *111*, 223–233. [CrossRef]
24. Chen, C.-C.; Chiang, K.-P.; Gong, G.-C.; Shiah, F.-K.; Tseng, C.-M.; Liu, K.-K. Importance of planktonic community respiration on the carbon balance of the East China Sea in summer. *Glob. Biogeochem. Cycles* **2006**, *20*, 1–14. [CrossRef]
25. Tseng, C.M.; Liu, K.-K.; Gong, G.-C.; Shen, P.-Y.; Cai, W.-J. CO_2 uptake in the East China Sea relying on Changjiang runoff is prone to change. *Geophys. Res. Lett.* **2011**, *38*, 1–6. [CrossRef]
26. Milliman, J.D.; Shen, H.T.; Yang, Z.S.; Mead, R.H. Transport and deposition of river sediment in the Changjiang estuary and adjacent continental shelf. *Cont. Shelf Res.* **1985**, *4*, 37–45. [CrossRef]
27. Edmond, J.M.; Spivack, A.; Grant, B.C.; Hu, M.H.; Chen, Z.; Chen, S.; Zeng, X. Chemical dynamics of the Changjiang estuary. *Cont. Shelf Res.* **1985**, *4*, 17–36. [CrossRef]
28. Zhang, J.; Liu, S.M.; Ren, J.L.; Wu, Y.; Zhang, G.L. Nutrient gradients from the eutrophic Changjiang (Yangtze River) Estuary to the oligotrophic Kuroshio waters and re-evaluation of budgets for the East China Sea Shelf. *Prog. Oceanogr.* **2007**, *74*, 449–478. [CrossRef]
29. Chen, C.-C.; Hsu, S.-C.; Jan, S.; Gong, G.-C. Episodic events imposed on the seasonal nutrient dynamics of an upwelling system off northeastern Taiwan. *J. Mar. Syst.* **2015**, *141*, 128–135. [CrossRef]
30. Chen, C.-T.A. The Kuroshio intermediate water is the major source of nutrients on the East China Sea continental shelf. *Oceanol. Acta* **1996**, *19*, 523–527.
31. Yang, D.; Yin, B.; Sun, J.; Zhang, Y. Numerical study on the origins and the forcing mechanism of the phosphate in upwelling areas off the coast of Zhejiang province, China in summer. *J. Mar. Syst.* **2013**, *123–124*, 1–18. [CrossRef]
32. Wang, W.; Yu, Z.; Song, X.; Wu, Z.; Yuan, Y.; Zhou, P.; Cao, X. The effect of Kuroshio Current on nitrate dynamics in the southern East China Sea revealed by nitrate isotopic composition. *J. Geophys. Res.* **2016**, *121*, 7073–7087. [CrossRef]
33. Chou, W.-C.; Sheu, D.D.; Chen, C.-T.A.; Wen, L.-S.; Yang, Y.; Wei, C.-L. Transport of the South China Sea subsurface water outflow and its influence on carbon chemistry of Kuroshio waters off southeastern Taiwan. *J. Geophys. Res.* **2007**, *112*, 1–11. [CrossRef]
34. Sheu, D.D.; Chou, W.-C.; Chen, C.-T.A.; Wei, C.-L.; Hsieh, H.-L.; Hou, W.-P.; Dai, M.H. Riding over the Kuroshio from the South to the East China Sea: Mixing and transport of DIC. *Geophys. Res. Lett.* **2009**, *36*, 251–254. [CrossRef]
35. Chen, C.-T.A. Distributions of nutrients in the East China Sea and the South China Sea connection. *J. Oceanogr.* **2008**, *64*, 737–751. [CrossRef]
36. Yang, D.Z.; Yin, B.S.; Hou, Y.J.; Sun, S.; Yu, Z.M.; Song, J.M.; Xu, L.J.; Yu, F.; Song, X.X.; Yu, R.C.; et al. Advance in research on Kuroshio intrusion and its ecological influence on the continental shelf of East China Sea. *Oceanol. Limnol. Sin.* **2007**, *48*, 1196–1207, (in Chinese with English abstract).
37. Dai, A.G.; Trenberth, K.E. Estimates of freshwater discharge from continents: Latitudinal and seasonal variations. *J. Hydrometeorol.* **2002**, *3*, 660–687. [CrossRef]

38. Stommel, H.M.; Yoshida, K. *Kuroshio: Its Physical Aspects*; University of Tokyo Press: Tokyo, Japan, 1972.
39. Yang, D.Z.; Yin, B.S.; Liu, Z.L.; Feng, X.R. Numerical study of the ocean circulation on the East China Sea shelf and a Kuroshio bottom branch northeast of Taiwan in summer. *J. Geophys. Res.* **2011**, *116*, C05015. [CrossRef]
40. Jan, S.; Yang, Y.J.; Wang, J.; Mensah, V.; Kuo, T.-H.; Chiou, M.-D.; Chern, C.-S.; Chang, M.-H.; Chien, H. Large variability of the Kuroshio at 23.75 degrees N east of Taiwan. *J. Geophys. Res.* **2015**, *120*, 1825–1840. [CrossRef]
41. Qiu, B.; Imasato, N. A Numerical Study on the Formation of the Kuroshio Counter Current and the Kuroshio Branch Current in the East China Sea. *Cont. Shelf Res.* **1990**, *10*, 165–184. [CrossRef]
42. Dickson, A.G.; Sabine, C.L.; Christian, J.R. *Guide to Best Practices for Ocean CO_2 Measurements*; North Pacific Marine Science Organization: Sidney, BC, Canada, 2007.
43. Zhai, W.D.; Zheng, N.; Huo, C.; Xu, Y.; Zhao, H.D.; Li, Y.W.; Zang, K.P.; Wang, J.Y.; Xu, X.M. Subsurface pH and carbonate saturation state of aragonite on the Chinese side of the North Yellow Sea: Seasonal variations and controls. *Biogeosciences* **2014**, *11*, 1103–1123. [CrossRef]
44. Fu, M.Z.; Wang, Z.L.; Li, Y.; Li, R.X.; Sun, P.; Wei, X.H.; Lin, X.Z.; Guo, J.S. Phytoplankton biomass size structure and its regulation in the Southern Yellow Sea (China): Seasonal variability. *Cont. Shelf Res.* **2009**, *29*, 2178–2194. [CrossRef]
45. Lewis, E.; Wallace, D.W.R. *Program Developed for CO_2 System Calculations*; Report ORNLrCDIAC-105; Carbon Dioxide Information Analysis Center, Oak Ridge National Laboratory: Oak Ridge, TN, USA, February 1998.
46. Mehrbach, C.; Culberson, C.H.; Hawley, J.E.; Pytkowicz, R.M. Measurement of apparent dissociation constants of carbonic acid in seawater at atmospheric pressure. *Limnol. Oceanogr.* **1973**, *18*, 897–907. [CrossRef]
47. Dickson, A.G.; Millero, F.J. A comparison of the equilibrium constants for the dissociation of carbonic acid in seawater media. *Deep Sea Res.* **1987**, *34*, 1733–1743. [CrossRef]
48. Dickson, A.G. Standard potential of the reaction: AgCl(s) + $1/2H_2$(g) = Ag(s) + HCl(aq) and the standard acidity constant of the ion $HSO4^-$ in synthetic seawater from 273.15 to 318.15 K. *J. Chem. Thermodyn.* **1990**, *22*, 113–127. [CrossRef]
49. Dickson, A.G. Thermodynamics of the dissociation of boric acid in synthetic seawater from 273.15 to 318.15 K. *Deep Sea Res. Part I* **1990**, *37*, 755–766. [CrossRef]
50. Bryan, J.R.; Riley, J.P.; Williams, P.J.L. Winkler procedure for making precise measurements of oxygen concentration for productivity and related studies. *J. Exp. Mar. Biol. Ecol.* **1976**, *21*, 191–197. [CrossRef]
51. Hung, J.-J.; Lin, P.-L.; Liu, K.-K. Dissolved and particulate organic carbon in the southern East China Sea. *Cont. Shelf Res.* **2000**, *20*, 545–569. [CrossRef]
52. Yuan, D.L.; Zhu, J.R.; Li, C.Y.; Hu, D.X. Cross-shelf circulation in the Yellow and East China Seas indicated by MODIS satellite observations. *J. Mar. Syst.* **2008**, *70*, 134–149. [CrossRef]
53. Chen, C.-T.A. Chemical and physical fronts in the Bohai, Yellow and East China seas. *J. Mar. Syst.* **2009**, *78*, 394–410. [CrossRef]
54. Chen, C.-T.A.; Wang, S.-L. A salinity front in the southern East China Sea separating the Chinese coastal and Taiwan Strait waters from Kuroshio waters. *Cont. Shelf Res.* **2006**, *26*, 1636–1653. [CrossRef]
55. Ichikawa, H.; Chaen, M. Seasonal variation of heat and freshwater transports by the Kuroshio in the East China Sea. *J. Mar. Syst.* **2000**, *24*, 119–129. [CrossRef]
56. Qi, J.F.; Yin, B.S.; Zhang, Q.L.; Yang, D.Z.; Xu, Z.H. Analysis of seasonal variation of water masses in East China Sea. *Chinese J. Oceanol. Limnol.* **2014**, *32*, 958–971. [CrossRef]
57. Sheu, D.D.; Lee, W.Y.; Wang, C.H.; Wei, C.L.; Chen, C.T.A.; Cherng, C.; Huang, M.H. Depth distribution of delta $\delta^{13}C$ of dissolved $\sum CO_2$ in seawater off eastern Taiwan: Effects of the Kuroshio current and its associated upwelling phenomenon. *Cont. Shelf Res.* **1996**, *16*, 1609–1619. [CrossRef]
58. Fuenzalida, R.; Schneider, W.; Garces-Vargas, J.; Bravo, L.; Lange, C. Vertical and horizontal extension of the oxygen minimum zone in the eastern South Pacific Ocean. *Deep Sea Res. Part II Top. Stud. Oceanogr.* **2009**, *56*, 1027–1038. [CrossRef]
59. Karstensen, J.; Stramma, L.; Visbeck, M. Oxygen minimum zones in the eastern tropical Atlantic and Pacific oceans. *Prog. Oceanogr.* **2008**, *77*, 331–350. [CrossRef]
60. Ulloa, O.; Pantoja, S. The oxygen minimum zone of the eastern South Pacific. *Deep Sea Res. Part II Top. Stud. Oceanogr.* **2009**, *56*, 987–991. [CrossRef]

61. Hung, J.-J.; Chen, C.-H.; Gong, G.-C.; Sheu, D.D.; Shiah, F.-K. Distributions, stoichiometric patterns and cross-shelf exports of dissolved organic matter in the East China Sea. *Deep Sea Res. Part II Top. Stud. Oceanogr.* **2003**, *50*, 1127–1145. [CrossRef]
62. Millero, F.J. Thermodynamics of the carbon dioxide system in the oceans. *Geochim. Cosmochim. Acta* **1995**, *59*, 661–677. [CrossRef]
63. Takahashi, T.; Sutherland, S.C.; Sweeney, C.; Poisson, A.; Metzl, N.; Tilbrook, B.; Bates, N.; Wanninkhof, R.; Feely, R.A.; Sabine, C.; et al. Global sea-air CO_2 flux based on climatological surface ocean *p*CO2 and seasonal biological and temperature effects. *Deep Sea Res. Part II Top. Stud. Oceanogr.* **2002**, *49*, 1601–1622. [CrossRef]
64. Chen, F.; Cai, W.-J.; Claudia, B.-N.; Wang, Y. Sea surface pCO_2-SST relationships across a cold-core cyclonic eddy: Implications for understanding regional variability and air-sea gas exchange. *Geophys. Res. Lett.* **2007**, *341*, 265–278.
65. Zhang, L.J.; Xue, L.; Song, M.Q.; Jiang, C.B. Distribution of the surface partial pressure of CO_2 in the southern Yellow Sea and its controls. *Cont. Shelf Res.* **2010**, *30*, 293–304. [CrossRef]
66. Yang, D.Z.; Yin, B.S.; Liu, Z.L.; Bai, T.; Qi, J.F.; Chen, H.Y. Numerical study on the pattern and origins of Kuroshio branches in the bottom water of southern East China Sea in summer. *J. Geophys. Res.* **2012**, *117*, C02014. [CrossRef]
67. Sarmiento, J.L.; Gruber, N. Carbon cycle. In *Ocean Biogeochemical Dynamics*; Sarmiento, J.L., Gruber, N., Eds.; Princeton University Press: Princeton, NJ, USA, 2006; pp. 318–358.
68. Zuo, J.L.; Song, J.M.; Yuan, H.M.; Li, X.G.; Li, N.; Duan, L.Q. Particulate nitrogen and phosphorus in the East China Sea and its adjacent Kuroshio waters and evaluation of budgets for the East China Sea Shelf. *Cont. Shelf Res.* **2016**, *131*, 1–11. [CrossRef]
69. Zhou, F.; Xue, H.; Huang, D.; Xuan, J.; Ni, X.; Xiu, P.; Hao, Q. Cross-shelf exchange in the shelf of the East China Sea. *J. Geophys. Res.* **2015**, *120*, 1545–1572. [CrossRef]